Cascaded higher-order soliton for non-adiabatic pulse compression

Qian Li,[1] J. Nathan Kutz,[2] and P. K. A. Wai[1,*]

[1]*Photonics Research Centre, Department of Electronic and Information Engineering, The Hong Kong Polytechnic University, Hung Hom, Hong Kong*
[2]*Department of Applied Mathematics, University of Washington, Seattle, Washington 98195-2420, USA*
**Corresponding author: enwai@polyu.edu.hk*

Received June 7, 2010; revised August 12, 2010; accepted August 13, 2010;
posted August 17, 2010 (Doc. ID 129676); published October 8, 2010

Non-adiabatic pulse compression of cascaded higher-order optical soliton is investigated. We demonstrate high degree compression of pulses with soliton orders $N=2$, 3, 4, and 5 in two or three nonlinear fibers with different second-order dispersion coefficients. Each fiber length is shorter than half of its soliton period. This compression technique has significant advantages over the widely reported adiabatic and higher-order soliton compression.

OCIS codes: 190.7110, 320.5520.

1. INTRODUCTION

The ability to robustly and routinely produce ultrashort pulses has led to transformative technologies in such diverse areas as telecommunications, photonics, and biological imaging. Ultrashort optical pulse sources are critical components for applications in which femtosecond or picosecond time resolution, high peak powers, and/or large optical bandwidths are required [1]. Ultrashort pulses are usually generated with mode-locked lasers. However, mode-locked lasers can be complex and costly, and the ultrashort pulses emitted from high-energy mode-locked laser sources are often chirped and/or limited to fairly low output powers. As an alternative, various pulse compression schemes have been proposed to generate ultrashort pulses with high-energy content. Pulse compressors based on nonlinear fiber optics can be classified into two broad categories: grating-fiber and soliton-effect compressors [2]. In a grating-fiber compressor, the input pulse is first propagated in the normal-dispersion fiber which imposes a nearly linear positive chirp on the pulse through a combination of self-phase modulation and group velocity dispersion (GVD), and then compressed externally using a grating pair. The grating pair provides the anomalous GVD for compression of positively chirped pulses. Grating-fiber compressors are useful for compressing pulses in the visible and near-infrared regions, while soliton-effect compressors work typically in the range from 1.3 to 1.6 μm [2]. For grating-fiber compressors, the compression factor can be estimated by $F_c \approx N/1.6$, where N is the soliton order [3]. Although in theory the compression factor can be increased by increasing the peak power of the incident pulse, it is limited in practice since the peak power should be kept below the Raman threshold to avoid the transfer of pulse energy to the Raman pulse. For the soliton-effect compression, two commonly considered techniques are the higher-order soliton compression scheme and the adiabatic pulse compression method. Unfortunately, each method suffers from significant technological drawbacks: the former from the generation of a large pedestal/background structure that contains a large portion of the pulse energy [4], and the latter from a limit on the compression factor and excessively long dispersion decreasing fiber (DDF) segments [5]. In this paper, a hybrid technique is proposed that takes advantage of the strength of both compression techniques while avoiding their drawbacks. Specifically, we theoretically study the cascaded N-soliton for non-adiabatic pulse compression in two or three nonlinear fibers with different constant anomalous dispersion coefficients. Very large compression factors can be achieved with the generation of a relatively small pedestal, making the technique competitive with current pulse compression technologies.

To be more specific about the performance of previous compression techniques using solitons, the higher-order (non-adiabatic) compression can be considered. In this case, large compression factors can be achieved, but it suffers from energy splitting between the desired compressed pulse and an undesired broad background. The resulting pulses are of poor quality unless reshaping techniques are used. In some of these techniques, such as the nonlinear intensity discrimination with nonlinear induced birefringence [6,7] or the nonlinear optical loop mirror (NOLM) [8], the suppression of pedestal can be achieved, but a great deal of energy is wasted. Another disadvantage with this technique is that the required input power is high and cannot be obtained directly from semiconductor lasers; thus an additional large gain optical amplification is necessary [5]. Optimum compression of an $N=15$ soliton can generate a compression factor of 60, but up to 80% of the pulse energy is contained in the pedestal component [4]. Thus it is a highly inefficient method, from an energy standpoint, for producing ultrashort pulses.

For the adiabatic pulse compression, the fundamental soliton is typically used in a dispersion map with monotonically decreasing dispersion along the propagation direction. If the dispersion decreases slowly enough, the soliton can self-adjust to maintain the balance between dispersion and nonlinearity by reducing its pulse width [9]. Generation of pulses of less than 200 fs duration has been demonstrated experimentally using DDFs [10–12]. The compression factor is determined by the ratio of input and output dispersion, and the input power requirement is significantly lower than that for the higher-order soliton compression. This compression scheme is attractive since in the compression process, the pulse maintains its transform-limited characteristics and generates much smaller pedestal compared to that in the higher-order soliton compression scheme. However, the drawback is that the maximum compression factor is limited to about 20, and the fiber length required for broad input pulse tends to be excessively long [5]. Further, DDFs can be rather expensive to procure or manufacture.

In order to incorporate the desirable features of both the higher-order soliton compression and adiabatic pulse compression while diminishing their inherent drawbacks, Pelusi and Liu proposed the higher-order soliton ($N\sim2$) compression in a DDF [5]. Increasing the soliton order to $N\sim2$ can reduce the required DDF length and increase the pulse compression factor without significant pedestal generation. An $N=2.1$ soliton in a linear profiled DDF with length equal to one soliton period gives a compression factor of 55 and corresponding pedestal energy of 30%. The same compression factor can only be achieved by the conventional higher-order soliton compression using an $N\sim13$ soliton, but the pedestal energy is as high as 75% [4].

Another attractive solution to achieve pulse compression is to utilize a highly dispersive nonlinear medium such as a fiber Bragg grating (FBG). The grating dispersion just outside the stop band is up to 6 orders of magnitude larger than that of silica fiber, making it a feasible technology for constructing a very short all-fiber compressor. The first experimental observation of nonlinear propagation effects in FBGs, resulting in nonlinear optical pulse compression and soliton propagation at 76% of the speed of light in a uniform medium, is reported in [13]. The adiabatic soliton compression in a non-uniform grating in which the dispersion decreases along the grating has also been proposed [14]. Recently, we demonstrate nearly chirp-free and pedestal-free pulse compression of linearly chirped self-similar pulses near the photonic bandgap (PBG) structure of FBGs [15]. Efficient pulse compression can be achieved with the exponentially decreasing dispersion. However, the fabrication of grating with exponentially decreasing dispersion is nontrivial, although almost any grating profile can be manufactured using the state-of-the-art grating-writing technique. The stepwise approximation of the exponentially decreasing dispersion profile normally requires more than six segments [15], which also creates complexity in this scheme. Furthermore, the maximum compression factor is limited by the width of the PBG structure [16]. Very recently, a high degree pulse compressor was reported based on the chirped two-soliton breather in the exponentially decreasing dispersion [17,18]. If the initial chirp is carefully chosen, pedestal-free, nearly chirp-free, and high degree compression can be realized.

Recently, soliton-effect compression to few-cycle durations has been studied both theoretically [19–21] and experimentally [22]. The possibility of sub-2-cycle soliton-effect pulse compression at 800 nm in photonic crystal fibers (PCFs) is numerically investigated [19]. Soliton compression to a 2 fs pulse width with a compression factor of up to 50 is demonstrated numerically for a dispersion profile typical of a small-core PCF [20]. By exploiting the broad region of the GVD and the large effective nonlinearity of photonic nanowires, soliton-effect self-compression of 70 fs down to 6.8 fs is demonstrated experimentally [22].

Despite significant technological progress, it remains of great interest to develop a compression technique capable of achieving both high-quality pulses and large compression factors. Ideally, the required input power should be low, the fiber length should be short, and the fabrication should be easy. The method proposed here achieves many of the desired properties of an ideal compressor. Specifically, by using cascaded N-solitons for non-adiabatic pulse compression in two or three nonlinear fibers with different constant anomalous dispersion coefficient, very large compression factors can be achieved with relatively small pedestals. The method requires low input powers in conjunction with short sections of constant dispersion fibers, all of which are technological components that are inexpensive and readily available.

The paper is organized as follows. N-soliton dynamics are discussed in Section 2. The numerical results for cascaded N-soliton compression will be presented in Subsection 3.A. The discussion on soliton robustness will be offered in Subsection 3.B. The influence of higher-order fiber effects will be given in Section 4. The advantages of the cascaded N-soliton compression and its promising applications will be highlighted in the discussion and conclusion in Section 5.

2. BACKGROUND

Optical pulses are typically modeled by reducing Maxwell's equations via high-frequency asymptotics. Several key assumptions are made in this analytical reduction including (i) quasi-monochromatic waves, (ii) a slowly varying envelope, and (iii) uni-directional one-dimensional wave propagation. For pulses longer than 1 ps in duration, the pulse propagation in nonlinear fibers is governed by the nonlinear Schrödinger (NLS) equation [23],

$$i\frac{\partial A}{\partial z}-\frac{\beta_2}{2}\frac{\partial^2 A}{\partial t^2}+\gamma|A|^2A=0, \tag{1}$$

where A is the slowly varying amplitude of the pulse envelope, z is the distance, t is the time in the pulses' frame of reference, β_2 is the second-order dispersion coefficient, and γ is the nonlinear coefficient. The soliton order N is defined as

$$N=\sqrt{L_D/L_N}, \tag{2}$$

where L_D and L_N are the dispersion and nonlinear lengths, respectively. The fundamental soliton arises for

$L_D = L_N$. For all higher-order solitons ($N > 1$), $|A|^2$ is periodic with the period

$$z_0 = \frac{\pi}{2} L_D. \tag{3}$$

Figure 1 shows the $N=2$-, 3-, 4-, and 5-soliton evolution over one period. As the pulse propagates along the fiber, it first contracts to a fraction of its initial width, splits into a multi-humped pulse, and then merges again, in a symmetric fashion, to recover the original shape at the end of soliton period $z = z_0$. In the conventional higher-order soliton compression, the fiber length is chosen so that the soliton pulse is at its highest peak during the evolution, which corresponds to the minimum pulse width. This gives the maximum compression factor possible in the higher-order soliton compression schemes. Indeed, the compressed pulse is much narrower than the initial pulse. However, the pulse is now accompanied by a potentially large pedestal. Specifically, the larger the soliton order, the larger the generated pedestal. For high-quality pulse compression, the pedestal must be minimized in order to suppress the deleterious interaction between the pedestal and compressed spike that occurs upon further propagation. The interaction leads to a host of undesirable periodic pulse reshaping effects [24] that are detrimental for optical communication applications.

The key idea of this paper is to consider switching the dispersion of the fiber at the maximal compression point so that the localized compressed pulse structure is now ready to be compressed again as a new higher-order soliton in the next fiber segment. Specifically, consider Fig. 1(a) which shows the evolution of an $N=2$ soliton. At a propagation distance of $z/z_0 = 0.5$, the pulse has been compressed, and its peak intensity increased by a factor of 4. The idea is to now make this new compressed pulse an $N=2$ soliton in a new fiber segment and compress the pulse again so that the intensity is again increased by another factor of 4. All that is required in this process is to determine the length of the fiber and the dispersion of the next fiber segment. Cascading higher-order solitons this way is a promising compression technology provided that the pedestal can be kept relatively small. This will be explored in the following sections.

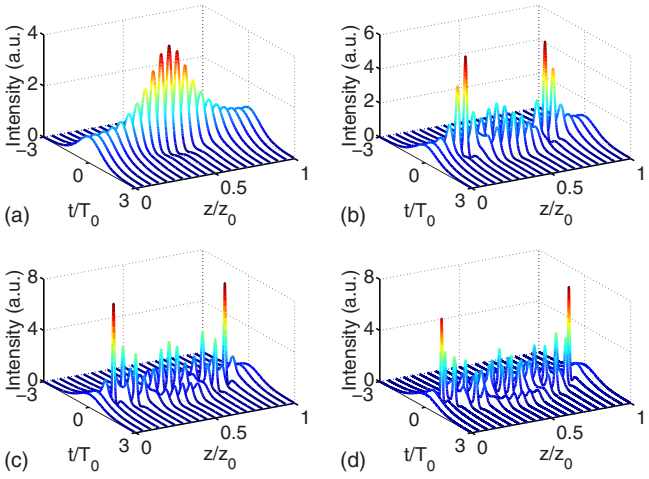

Fig. 1. (Color online) Soliton evolution over one period for (a) $N=2$, (b) $N=3$, (c) $N=4$, and (d) $N=5$. Note that the higher the soliton order, the higher the compression and pedestal formation.

3. PULSE COMPRESSION

A. Cascaded *N*-Soliton Compression

For the proposed two-stage N-soliton compression, the initial pulse is a chirp-free hyperbolic secant pulse $N_1 \operatorname{sech}(\tau)$, where τ is the normalized time, and N_1 is the soliton order in the first fiber. The output of the first fiber is launched into a second fiber with a different dispersion coefficient, and the soliton order in the second fiber is N_2. Consequently, we have

$$N_1^2 = T_{01}^2 \gamma P_1 / |\beta_{21}|, \quad N_2^2 = T_{02}^2 \gamma P_2 / |\beta_{22}|, \tag{4}$$

where $T_{01,02}, P_{1,2}, \beta_{21,22}$ are the initial pulse width parameter, peak power, and second-order dispersion in the first and second fibers, respectively. Since the input of the second fiber is not an exact hyperbolic secant shape, T_{02} is decided by the pulse fitting with a sech^2 pulse having the same peak power and full width at half-maximum (FWHM) intensity. Here, we assume the nonlinear coefficient γ is same for the first and second fibers. For higher-order soliton formation, both β_{21} and β_{22} are negative. First, we consider the case for which $N_1 = N_2 = N$. Figures 2(a) and 2(b) show the peak power evolution in the first fiber within one soliton period z_{01}. The solid and dashed curves in Fig. 2(a) represent $N=2$ and $N=3$, respectively. The solid and dashed curves in Fig. 2(b) represent $N=4$ and $N=5$, respectively. Figures 2(c) and 2(d) show the peak power evolution in the second fiber within one soliton period z_{02}. The solid and dashed curves in Fig. 2(c) represent $N=2$ and $N=3$, respectively. The solid and dashed curves in Fig. 2(d) represent $N=4$ and $N=5$, respectively. Note that the maximum peak power corresponds to a minimum pulse width. For each different N,

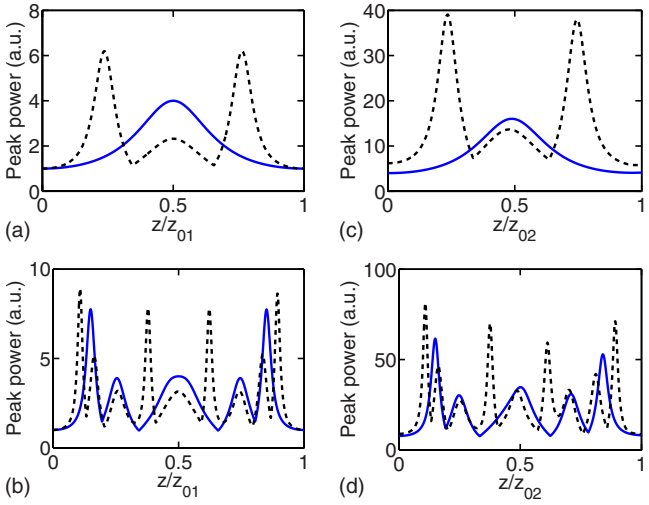

Fig. 2. (Color online) (a) and (b) show the peak power evolution in the first fiber within one soliton period z_{01}. The solid and dashed curves in (a) represent $N=2$ and $N=3$, respectively. The solid and dashed curves in (b) represent $N=4$ and $N=5$, respectively. (c) and (d) show the peak power evolution in the second fiber within one soliton period z_{02}. The solid and dashed curves in (c) represent $N=2$ and $N=3$, respectively. The solid and dashed curves in (d) represent $N=4$ and $N=5$, respectively.

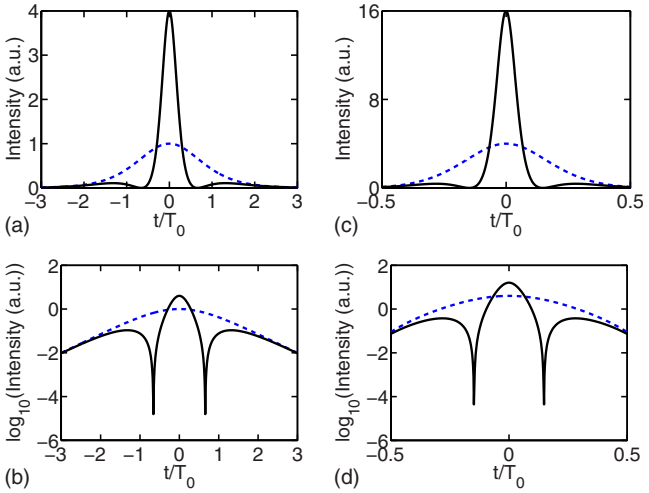

Fig. 3. (Color online) Pulse shapes where compression is maximized in both the first and second fibers for $N=2$. The dashed and solid curves in (a) and (b) represent the input and output pulses of the first fiber in (a) linear and (b) logarithmic scales. The dashed and solid curves in (c) and (d) represent the input and output pulses of the second fiber in (c) linear and (d) logarithmic scales.

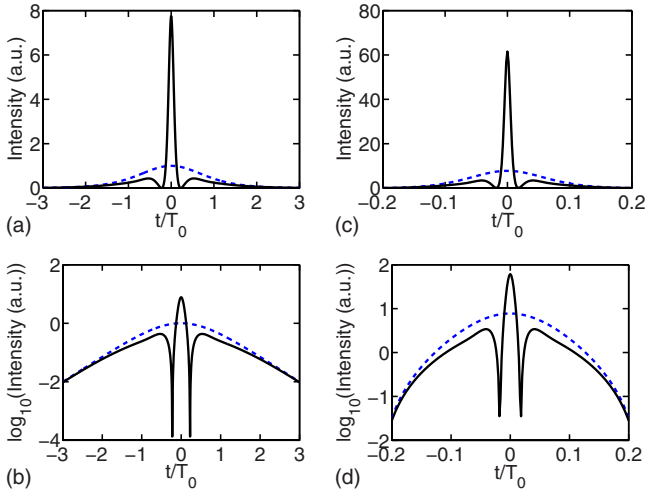

Fig. 5. (Color online) Pulse shapes where compression is maximized in both the first and second fibers for $N=4$. The dashed and solid curves in (a) and (b) represent the input and output pulses of the first fiber in (a) linear and (b) logarithmic scales. The dashed and solid curves in (c) and (d) represent the input and output pulses of the second fiber in (c) linear and (d) logarithmic scales.

the peak power evolutions in the first fiber (one soliton period) and the second fiber (one soliton period) are quite similar. For the two-stage N-soliton compression, the pulse with a minimum pulse width in the first fiber is used as the input of the second fiber. Figures 3(a) and 3(b) show the pulse shapes where compression is maximized in the first fiber when $N=2$. The dashed and solid curves represent the input and output pulses of the first fiber in both linear and logarithmic scales. The intensity enhancement by a factor of 4 is clearly illustrated. Figures 3(c) and 3(d) show the pulse shapes where compression is maximized in the second fiber using a fiber dispersion corresponding to an $N=2$ fitted input soliton. The dashed and solid curves represent the input and output pulses of the second fiber again in linear and logarithmic scales. Similarly, Figs. 4–6 show the pulse shapes where compression is maximized in both the first and second fibers for the $N=3$, 4, and 5 solitons, respectively. With the increase in the soliton order N, pulse compression becomes more effective, but at the price of increased pedestal generation. The specific details of the compression factor and pedestal energy are given in Table 1.

Table 1 gives a comprehensive evaluation of the compression factor and pedestal energy in the first and second fibers for the proposed two-stage N-soliton compression. The pedestal energy is defined as the relative difference between the total energy of the transmitted

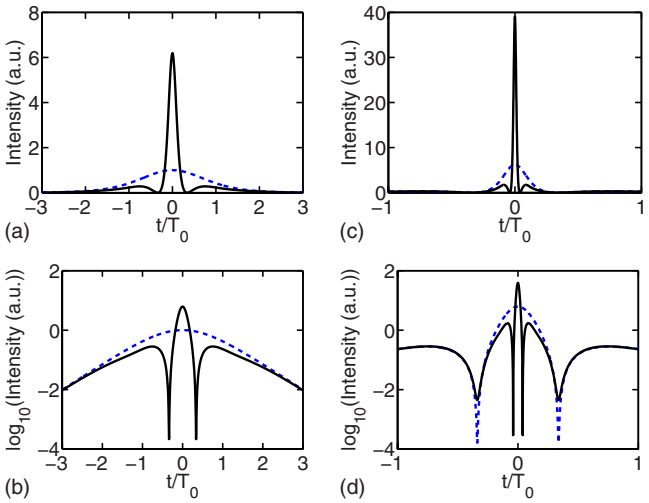

Fig. 4. (Color online) Pulse shapes where compression is maximized in both the first and second fibers for $N=3$. The dashed and solid curves in (a) and (b) represent the input and output pulses of the first fiber in (a) linear and (b) logarithmic scales. The dashed and solid curves in (c) and (d) represent the input and output pulses of the second fiber in (c) linear and (d) logarithmic scales.

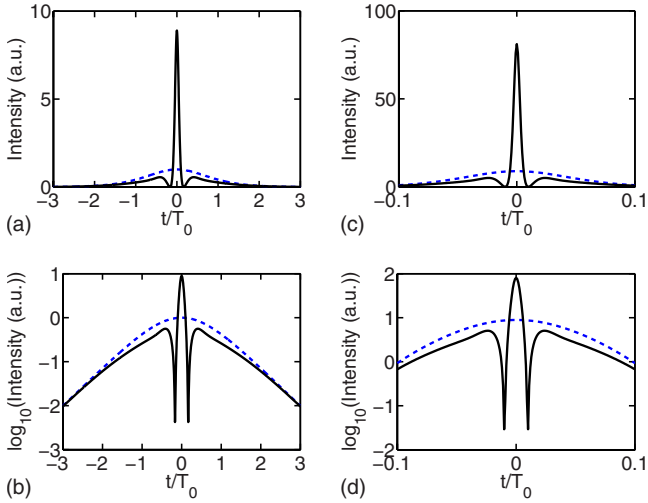

Fig. 6. (Color online) Pulse shapes where compression is maximized in both the first and second fibers for $N=5$. The dashed and solid curves in (a) and (b) represent the input and output pulses of the first fiber in (a) linear and (b) logarithmic scales. The dashed and solid curves in (c) and (d) represent the input and output pulses of the second fiber in (c) linear and (d) logarithmic scales.

Table 1. Compression Factor and Pedestal (%) in the First and Second Fibers for Two-Stage *N*-Soliton Compression

	$N=2$		$N=3$		$N=4$		$N=5$	
	First	Second	First	Second	First	Second	First	Second
Comp. factor	4.4	19.7	8.4	70.8	12.5	158.4	17.0	283.9
Pedestal (%)	9.8	18.8	26.0	44.8	38.0	61.1	46.9	71.3

pulse and the energy of a hyperbolic secant pulse having the same peak power and width as those of the transmitted pulse [25], i.e.,

$$\text{Pedestal}\ (\%) = \frac{|E_{\text{total}} - E_{\text{sech}}|}{E_{\text{total}}} \times 100\%. \tag{5}$$

Note that the energy of a hyperbolic secant pulse with peak power P_{peak} and pulse width FWHM is given by

$$E_{\text{sech}} = 2P_{\text{peak}}\frac{\text{FWHM}}{1.763}. \tag{6}$$

We note that with the increase in the soliton order N, the compression factor becomes larger, but the pedestal becomes more pernicious. For each different N, the compression factor after the second fiber is almost the square of the compression factor after the first fiber, and the pedestal in the second fiber is smaller than twice of the pedestal in the first fiber. This suggests that the pedestal plays only a small role in the compression enhancement. As mentioned in the introduction, in the conventional higher-order soliton compression, for a pulse compression factor of 60, the pedestal energy was as high as 80%. In our two-stage third-order soliton compression, the compression factor is 70.8 and the pedestal is 44.8%, which is much better than the conventional higher-order soliton compression. Higher soliton orders ($N>3$) can also be used in the two-stage compression, and it is without significant increase in the pedestal. The two-stage fifth-order soliton compression gives an impressive compression factor of 283.9 and corresponding pedestal energy of 71.3%. The specific fiber components required for generating such a performance are given in Table 2. Specifically, details of the fiber design in the two-stage N-soliton compression are explicitly presented, where $\beta_{21},\beta_{22},L_1,L_2$ represent the second-order dispersion of the first and second fibers, and the length of the first and second fibers, respectively. The dispersion coefficient of the second fiber is always smaller than the dispersion coefficient of the first fiber. With the increase in N, the ratio of the dispersion coefficients in the second and first fibers, $|\beta_{22}|/|\beta_{21}|$, becomes smaller, and the maximum compression happens earlier compared to the soliton period (L_1/z_{01} or L_2/z_{02} becomes smaller with the increase in N). For each different N, $L_1/z_{01}\sim L_2/z_{02}$. For example, for $N=2$, the maximum compression in the first and second fibers occur at $L_1=0.5z_{01}$, and $L_2=0.486z_{02}$, respectively; for $N=5$, the maximum compression in the first and second fiber occur at $L_1=0.108z_{01}$, and $L_2=0.109z_{02}$, respectively. For the optimized two-stage N-soliton compression, the first or second fiber length (L_1 or L_2) is always smaller than the half of soliton period of the first or second fiber ($z_{01}/2$ or $z_{02}/2$), which makes for a compact compression scheme. We can also use two-stage higher-order soliton compression when $N_1\neq N_2$. Table 3 lists the compression factor and pedestal for $N_1=2$, $N_2=3$, 4, 5. For the combination of $N_1=2$ and $N_2=3$, the final compression factor and pedestal are 37.5 and 32.8%, respectively, and the performance is between that of $N_1=N_2=2$ and that of $N_1=N_2=3$. We have similar observations for $N_1=2$, $N_2=4$, 5. Table 4 gives the second fiber design in the two-stage N-soliton compression when $N_1=2$, $N_2=3$, 4, 5. The first fiber follows the design in Table 2.

The two-stage N-soliton compression is very attractive in comparison with current compression schemes and techniques. We also investigated the performance of a three-stage N-soliton compression. As an illustration, we consider the case where $N_1=N_2=N_3=N$, where N_1,N_2,N_3 are soliton orders in the first, second, and third fibers, respectively. The fiber length is optimized to have maximum compression in all three fibers. The first and second fibers follow the design in Table 2. The third fiber dispersion coefficient β_{23} and length L_3 are given in Table 5. Figure 7 gives the final pulse shape for a three-stage second-order soliton compressor, where the dashed and solid curves represent the input and output pulses of the third fiber in linear and logarithmic scales. The final compres-

Table 2. Fiber Design in Two-Stage *N*-Soliton Compression

	$N=2$	$N=3$	$N=4$	$N=5$
$\lvert\beta_{22}\rvert/\lvert\beta_{21}\rvert$	0.204	0.0884	0.0496	0.0316
L_1/z_{01}	0.5	0.237	0.149	0.108
L_2/z_{02}	0.486	0.235	0.150	0.109

Table 3. Compression Factor and Pedestal (%) in the Second Fiber when $N_1=2$, $N_2=3$, 4, 5

$N_1=2$	$N_2=3$	$N_2=4$	$N_2=5$
Comp. factor after second fiber	37.5	56.1	75.1
Pedestal (%)	32.8	43.6	51.5

Table 4. Second Fiber Design in Two-Stage *N*-Soliton Compression when $N_1=2$, $N_2=3$, 4, 5

$N_1=2$	$N_2=3$	$N_2=4$	$N_2=5$
$\lvert\beta_{22}\rvert/\lvert\beta_{21}\rvert$	0.0904	0.0508	0.0326
L_2/z_{02}	0.235	0.150	0.108

Table 5. Third Fiber Design in Three-Stage *N*-Soliton Compression

	$N=2$	$N=3$
$\lvert\beta_{23}\rvert/\lvert\beta_{21}\rvert$	0.0416	0.0078
L_3/z_{03}	0.487	0.235

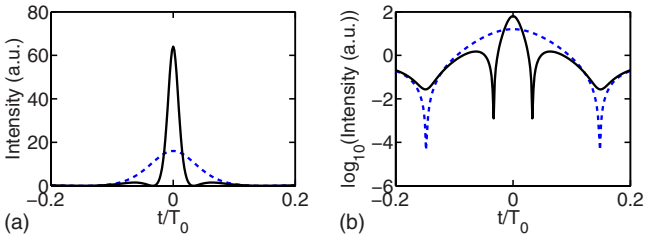

Fig. 7. (Color online) Pulse shapes where compression is maximized in the first, second, and third fibers for three-stage second-order soliton compression. The dashed and solid curves represent the input and output pulses of the third fiber in (a) linear and (b) logarithmic scales.

sion factor and pedestal content are 87.5 and 26.8%, respectively. The performance of the three-stage second-order soliton compression is better than that of the two-stage third-order soliton compression. Figure 8 gives the final pulse shape for three-stage third-order soliton compression, where the dashed and solid curves represent the input and output pulses of the third fiber in linear and logarithmic scales. The final compression factor and pedestal are 599.7 and 58.8%, respectively. The performance of the three-stage third-order soliton compression is better than that of the two-stage fourth-order soliton compression. Table 5 gives the design of the third fiber in the three-stage N-soliton compression for $N=2$ and $N=3$. Among the three fibers, the third fiber has the smallest dispersion coefficient. The maximum compression in the second and third fibers happens almost at same location $L_2/z_{02} \sim L_3/z_{03}$. The performance of the cascaded N-soliton compression scheme is quite exemplary, with an almost 4 orders of magnitude compression and only approximately 60% pedestal energy generated. The NOLM, consisting of a fiber directional coupler with its output ports spliced, has been successful in demonstrating pedestal suppression of optical pulses [26]. For the final compressed pulse in the three-stage third-order soliton compression, Figs. 8(c)–8(f) show the pulse shapes and spectra with and without the use of NOLM, where the spectrum corresponds to the input pulse width parameter $T_0=60$ ps. The dashed and solid curves in Figs. 8(c) and 8(d) represent the compressed pulses with and without the use of NOLM in linear [Fig. 8(c)] and logarithmic [Fig. 8(d)] scales. The unwanted pedestal has again been suppressed effectively. Figure 8(e) shows the spectrum of the final compressed pulse without NOLM, while Fig. 8(f) shows the spectrum of the compressed pulse with NOLM. The spike in the middle of the spectrum is the residual pedestal. Here, we define the spectral width to be the full width at half-maximum intensity where the spike is ignored in the spectrum. Figure 8(e) shows a center spike, i.e., the pedestal component. The spectral width in Fig. 8(f) is 24.7 nm.

B. Soliton Robustness

The above results demonstrated the effective compression by using two- or three-stage N-soliton. The input pulse has an ideal hyperbolic secant pulse shape. The peak power is carefully chosen to have the second-, third-,

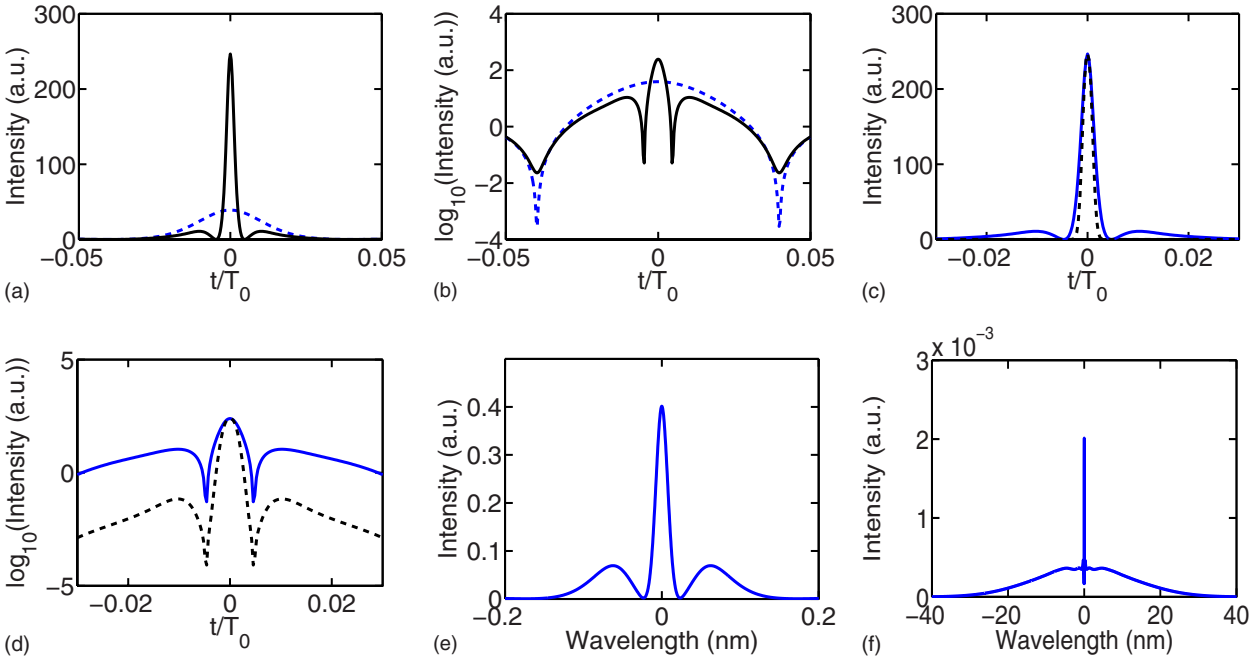

Fig. 8. (Color online) Pulse shapes where compression is maximized in the first, second, and third fiber for three-stage third-order soliton compression. The dashed and solid curves represent the input and output pulses of the third fiber in (a) linear and (b) logarithmic scales. Compressed pulse shapes with (dashed curve) and without (solid curve) the use of NOLM in (c) linear and (d) logarithmic scales for three-stage third-order soliton compression. (e) Spectrum of compressed pulse without NOLM. (f) Spectrum of compressed pulse with NOLM.

Table 6. Compression Factor and Pedestal (%) of the Compressed Pulse in the First and Second Fibers for Two-Stage *N*-Soliton Compression when *N*=2.5, 3.5, and 4.5

	N=2.5		*N*=3.5		*N*=4.5	
	First	Second	First	Second	First	Second
Comp. factor	6.4	40.5	10.4	123.0	14.6	216.8
Pedestal (%)	18.4	33.5	32.5	49.6	42.8	66.9

Table 7. Fiber Design in Two-Stage *N*-Soliton Compression when *N*=2.5, 3.5, and 4.5

	N=2.5	*N*=3.5	*N*=4.5
$\lvert\beta_{22}\rvert/\lvert\beta_{21}\rvert$	0.128	0.0648	0.0391
L_1/z_{01}	0.325	0.184	0.125
L_2/z_{02}	0.310	0.184	0.126

fourth-, or fifth-order soliton. Because of its practical application, it is critical to study the influence of peak power and non-hyperbolic-secant pulse shapes. First, we investigate the two-stage *N*-soliton compression when *N* is not an integer. Table 6 gives the compression factor and pedestal in the first and second fibers for two-stage *N*-soliton compression when *N*=2.5, 3.5, and 4.5. Table 7 gives the fiber design in two-stage *N*-soliton compression when *N* =2.5, 3.5, and 4.5. Note that for the two-stage *N*-soliton compression when *N*=2.5 (3.5, 4.5), the compression factor and pedestal are almost the average of the results of *N*=2 and *N*=3 (*N*=3 and *N*=4, *N*=4 and *N*=5).

Additionally, we consider the compression of a Gaussian input given by

$$A(0,t) = N_1 \exp(-t^2/T_0^2/2), \tag{7}$$

where N_1 is defined as $N_1^2 = T_0^2\gamma P_1/|\beta_{21}|$. T_0 and P_1 are the pulse width parameter and peak power of Gaussian input pulse. β_{21} and γ are the dispersion and nonlinear coefficients of the first fiber. Similar to the two-stage *N*-soliton compression, the fiber length is optimized to have maximum compression in both the first and second fibers in the two-stage *N*-Gaussian compression. After the first fiber, the Gaussian shaped pulse has evolved into a nearly hyperbolic secant shaped profile. The soliton order in the second fiber N_2 is $N_2^2 = (\mathrm{FWHM}/1.763)^2\gamma P_2/|\beta_{22}|$, where FWHM and P_2 are the full width at half-maximum intensity and peak power of the input pulse to the second fiber, respectively. The parameters β_{22} and γ are the dispersion and nonlinear coefficients of the second fiber. Here, we still use $N_1 = N_2 = N$. Tables 8 and 9 give the compression factor, pedestal, and fiber design for the two-stage *N*-Gaussian compression. For the two-stage *N*-Gaussian compression, the compression factor/pedestal is a little smaller than that of the two-stage *N*-soliton compression; the maximum compression in the first fiber happens at a shorter length (L_1/z_{01}) compared to the maximum compression in the first fiber of the two-stage *N*-soliton compression, and the maximum compression in the second fiber happens at almost the same location (L_2/z_{02}) compared to the maximum compression in the second fiber of the two-stage *N*-soliton compression.

4. HIGHER-ORDER EFFECTS

The results presented so far were based on an ideal fiber model [Eq. (1)] that ignores all the higher-order temporal effects. The advantage is that the results are generalized and may be denormalized to correspond to any arbitrary physical parameter, such as input pulse width, fiber dispersion and nonlinearity coefficients, and fiber length. However, for ultrashort optical pulses ($T_0 < 1$ ps), it is necessary to include higher-order dispersion and nonlinear effects, and the general NLS equation takes the form [23]

$$\frac{\partial A}{\partial z} + \frac{i\beta_2}{2}\frac{\partial^2 A}{\partial t^2} - \frac{\beta_3}{6}\frac{\partial^3 A}{\partial t^3} = i\gamma\left[|A|^2 A + \frac{i}{\omega_0}\frac{\partial}{\partial t}(|A|^2 A) - T_R A\frac{\partial |A|^2}{\partial t}\right], \tag{8}$$

where the second and third terms on the right-hand side of Eq. (8) represent the effect of self-steepening and intrapulse Raman scattering, respectively. Here, we assume that the pulse is wide enough to contain many optical cycles (pulse width > 100 fs), and the slope of the Raman gain spectrum varies linearly with frequency in the vicinity of the carrier frequency as shown in Eq. (8). In the following examples, the second-order dispersion of the first fiber is $\beta_{21} = -20$ ps^2/km; the third-order dispersion of the first and second fibers is $\beta_3 = 0.1$ ps^3/km; the center angular frequency is $\omega_0 = 2\pi c/\lambda_c$, where $\lambda_c = 1.55$ μm; and the slope of Raman gain is $T_R = 3$ fs. The nonlinear parameter is defined as $\gamma = n_2\omega_0/cA_{\mathrm{eff}}$, where n_2 is the nonlinear index coefficient, c is the light speed, and A_{eff} is the effective

Table 8. Compression Factor and Pedestal (%) in the First and Second Fibers for *N*-Gaussian Compression

	N=2		*N*=3		*N*=4		*N*=5	
	First	Second	First	Second	First	Second	First	Second
Comp. factor	3.92	17.46	7.85	66.39	11.99	152.16	16.2	275.74
Pedestal (%)	3.9	13.45	17.61	38.56	29.63	55.94	39.05	67.18

Table 9. Fiber Design in Two-Stage *N*-Gaussian Compression

	$N=2$	$N=3$	$N=4$	$N=5$
$\lvert\beta_{22}\rvert/\lvert\beta_{21}\rvert$	0.205	0.0879	0.0491	0.0315
L_1/z_{01}	0.465	0.227	0.145	0.106
L_2/z_{02}	0.484	0.236	0.149	0.108

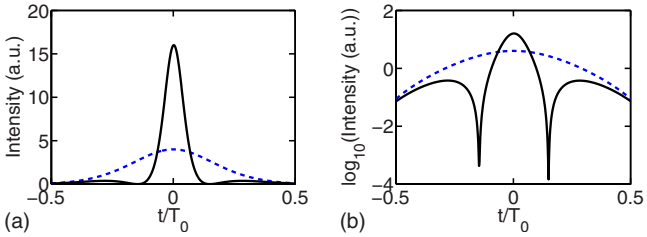

Fig. 9. (Color online) The dashed and solid curves represent the input and output pulses of second fiber in (a) linear and (b) logarithmic scales for two-stage second-order soliton compression where initial pulse width parameter $T_0=20$ ps.

mode area. Typically, A_{eff} can vary in the range of $1-100\ \mu\text{m}^2$ in the 1.5 μm region. As a result, γ takes values in the range $1-100\ \text{W}^{-1}/\text{km}$ if $n_2=2.6\times10^{-20}\ \text{m}^2/\text{W}$ is used. For the two-stage second-order soliton compression, the length of the first fiber is $L_1=15.7$ km, the length of the second fiber is $L_2=3.8$ km, and the second-order dispersion of the second fiber is $\beta_{22}=-4.07\ \text{ps}^2/\text{km}$ ($D\sim3$ ps/km nm). We suggest the use of PCF for the second fiber. The dispersive properties of PCFs are very sensitive to the air-hole diameter and the hole-to-hole spacing [27], which indicates an attractive property of great controllability of chromatic dispersion in the PCF. Controllability of chromatic dispersion is a very important problem in optical communication systems [28], dispersion compensation [29], and nonlinear optics [30,31]. So far, various PCFs with remarkable dispersion properties have been studied both experimentally and numerically [32,33]. For the example here, the first fiber uses typical parameters of standard silica fibers, and the second fiber with $\beta_{22}=-4.07\ \text{ps}^2/\text{km}$ ($D\sim3$ ps/km nm) may use a proposed fiber design with a dispersion value not larger than 5 ps/km nm around 1.5 μm [34]. Moreover, with the state-of-the-art fiber fabrication technique, our proposed fiber should be easily manufactured. Figures 9–12 show the two-stage higher-order soliton compression when the initial pulse width parameter $T_0=20$ ps for $N=2$, 3, 4, and 5, respectively. The fibers follow the design in Table 2. Pulse

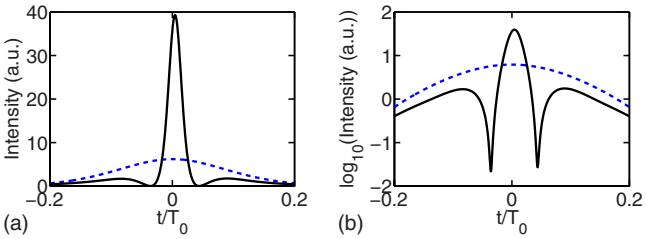

Fig. 10. (Color online) Dashed and solid curves represent the input and output pulses of second fiber in (a) linear and (b) logarithmic scales for two-stage third-order soliton compression where initial pulse width parameter $T_0=20$ ps.

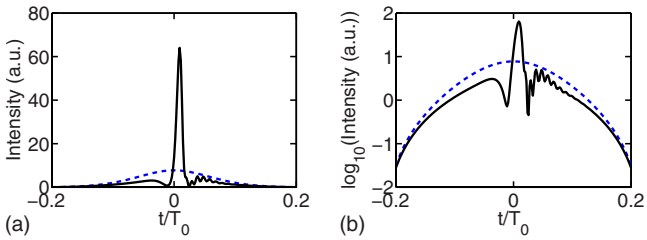

Fig. 11. (Color online) Dashed and solid curves represent the input and output pulses of second fiber in (a) linear and (b) logarithmic scales for two-stage fourth-order soliton compression where initial pulse width parameter $T_0=20$ ps.

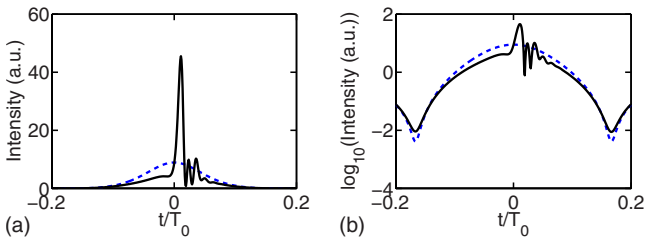

Fig. 12. (Color online) Dashed and solid curves represent the input and output pulses of second fiber in (a) linear and (b) logarithmic scales for two-stage fifth-order soliton compression where initial pulse width parameter $T_0=20$ ps.

compression in the first fiber is not shown here, because it is very close to the results without higher-order effects. The dashed and solid curves in Figs. 9–12 represent the input and output pulses of the second fiber in linear and logarithmic scales. For $N=2$ (Fig. 9) and $N=3$ (Fig. 10), the higher-order effects are not obvious. For $N=4$ (Fig. 11) and $N=5$ (Fig. 12), we can clearly see the higher-order effects: oscillations near the trailing edge of the pulse due to a positive third-order dispersion, a steeper trailing edge due to self-steepening effect, and a temporal shift of the pulse position due to intrapulse Raman scattering. Table 10 gives the compression factor and pedestal energy (in percent) of the compressed pulse in the second fiber. Comparing Tables 1 and 10, we note that the results including higher-order effects are very close to the results without higher-order effects when $N=2$ and $N=3$, but we can see a clear difference between the two when $N=4$ and $N=5$. The two-stage $N=4$ soliton compression gives a compression factor of 174.4 and corresponding pedestal of 76.5% if higher-order effects are included, while the two-stage $N=4$ soliton compression gives a compression factor of 158.4 and corresponding pedestal of 61.1% if higher-order effects are ignored. The two-stage $N=5$ soliton compression gives a compression factor of 177.4 and corresponding pedestal of 74.4% if higher-order effects are included, while the two-stage $N=5$ soliton compression gives a compression factor of 283.9 and corresponding pedestal of 71.3% if higher-order effects are ignored.

Table 10. Compression Factor and Pedestal (%) of the Compressed Pulse in the Second Fiber

	$N=2$	$N=3$	$N=4$	$N=5$
Comp. factor	19.7	71.5	174.4	177.4
Pedestal (%)	18.8	45.1	76.5	74.4

5. DISCUSSION AND CONCLUSIONS

A detailed investigation of a cascaded higher-order soliton compression scheme was presented. The results show clear and distinct advantages over the standard methods of adiabatic pulse compression, higher-order soliton compression, and higher-order soliton compression in DDF. Specifically, the cascaded higher-order soliton compression can achieve a very large compression factor using two or three nonlinear fibers with different constant anomalous dispersion coefficients. Each fiber length is shorter than half of its soliton period. The two-stage fifth-order soliton compression gives a compression factor of 284 and corresponding pedestal of 71%. The three-stage second-order soliton compression gives a compression factor of 87 and corresponding pedestal of 27%. The three-stage third-order soliton compression gives a compression factor of 600 and corresponding pedestal of 59%. These results are highly favorable when compared to the standard techniques previously used, thus suggesting that the cascaded higher-order soliton compression technique is a promising technology that is easy to implement with current technological components.

In terms of compression factor and pedestal energy, the cascaded higher-order soliton compression clearly provides the best performance among the four compression techniques. Moreover, the fabrication of fibers with different constant dispersion segments is much easier compared to the fabrication of DDFs. Specifically, PCFs offer greatly enhanced design freedom, such as the precise control of the chromatic dispersion, compared to standard optical fibers [35]. With fiber taping technologies and the use of PCF becoming commonplace, we anticipate the experimental realization of the cascaded N-soliton compression in the near future.

We also want to point out the obvious spectral broadening in the cascaded N-soliton compression. The initial hyperbolic secant pulse with $T_0=60$ ps has a spectral width of only 0.023 nm. After the three-stage $N=3$ soliton compression, the spectral width is 24.7 nm [Fig. 8(f)], corresponding to a spectral broadening factor of 1057. Ultrabroadband light can be generated if a shorter initial pulse is used. We believe that the cascaded N-soliton can also contribute to the area of supercontinuum generation.

Thus we have demonstrated that the cascaded higher-order soliton compression in two or three nonlinear fibers with different dispersion coefficients can achieve both high-quality compression and large compression factors. The two- or three-stage higher-order soliton compression can greatly increase the compression factor and lower the required input peak power without incurring significant degradation in the pulse quality. The cascaded N-soliton may have wide applications due to the ultrashort pulse generation and associated ultrabroadband generation.

ACKNOWLEDGMENTS

The authors acknowledge the support of The Hong Kong Polytechnic University (project J-BB9M), J. N. Kutz's support from the National Science Foundation (NSF) (DMS-0604700), and the U.S. Air Force Office of Scientific Research (AFOSR) (FA9550-09-0174).

REFERENCES

1. J. C. Diels and W. Rudolph, *Ultrashort Laser Pulse Phenomena* (Academic, 1998).
2. G. P. Agrawal, *Applications of Nonlinear Fiber Optics* (Academic, 2001).
3. W. J. Tomlinson, R. H. Stolen, and C. V. Shank, "Compression of optical pulses by self-phase modulation in fibers," J. Opt. Soc. Am. B **1**, 139–149 (1984).
4. K. C. Chan and H. F. Liu, "Short pulse generation by higher order soliton-effect compression: Effects of optical fiber characteristics," IEEE J. Quantum Electron. **31**, 2226–2235 (1995).
5. M. D. Pelusi and H. F. Liu, "Higher order soliton pulse compression in dispersion-decreasing optical fibers," IEEE J. Quantum Electron. **33**, 1430–1439 (1997).
6. R. H. Stolen, J. Botineau, and A. Ashkin, "Intensity discrimination of optical pulses with birefringent fibers," Opt. Lett. **7**, 512–514 (1982).
7. J. L. Tapié and G. Mourou, "Shaping of clean, femtosecond pulses at 1.053 μm for chirped pulse amplification," Opt. Lett. **17**, 136–138 (1992).
8. N. J. Doran and D. Wood, "Nonlinear-optical loop mirror," Opt. Lett. **13**, 56–58 (1988).
9. B. J. Eggleton, G. Lenz, and N. M. Litchinitser, "Optical pulse compression schemes that use nonlinear Bragg gratings," Fiber Integr. Opt. **19**, 383–421 (2000).
10. S. V. Chernikov, E. M. Dianov, D. J. Richardson, and D. N. Payne, "Soliton pulse compression in dispersion decreasing fiber," Opt. Lett. **18**, 476–478 (1993).
11. M. J. Guy, S. V. Chernikov, J. R. Taylor, D. G. Moodie, and R. Kashyap, "200 fs soliton pulse generation at 10 GHz through nonlinear compression of transform-limited pulses from an electroabsorption modulator," Electron. Lett. **31**, 740–741 (1995).
12. M. Nakazawa, E. Yoshida, H. Kubota, and Y. Kimura, "Generation of a 170 fs, 10 GHz transform-limited pulse train at 1.55 μm using a dispersion decreasing, erbium-doped active soliton compressor," Electron. Lett. **30**, 2038–2040 (1994).
13. B. J. Eggleton, R. E. Slusher, C. M. de Sterke, P. A. Krug, and J. E. Sipe, "Bragg grating solitons," Phys. Rev. Lett. **76**, 1627–1630 (1996).
14. G. Lenz and B. J. Eggleton, "Adiabatic Bragg soliton compression in nonuniform grating structures," J. Opt. Soc. Am. B **15**, 2979–2985 (1998).
15. Q. Li, K. Senthilnathan, K. Nakkeeran, and P. K. A. Wai, "Nearly chirp-and pedestal-free pulse compression in nonlinear fiber Bragg gratings," J. Opt. Soc. Am. B **26**, 432–443 (2009).
16. Q. Li, P. K. A. Wai, K. Senthilnathan, and K. Nakkeeran, "Modeling self-similar optical pulse compression in nonlinear fiber Bragg gratings using the coupled mode equations" (submitted to J. Lightwave Technol.).
17. K. Senthilnathan, K. Nakkeeran, Q. Li, and P. K. A. Wai, "Chirped higher order solitons" (submitted to J. Mod. Opt.).
18. K. Senthilnathan, K. Nakkeeran, Q. Li, and P. K. A. Wai, "Chirped optical solitons: High degree pulse compression," in *Proceedings of OptoElectronics and Communications Conference* (2009), paper FG2.
19. M. V. Tognetti and H. M. Crespo, "Sub-two-cycle soliton-effect pulse compression at 800 nm in photonic crystal fibers," J. Opt. Soc. Am. B **24**, 1410–1415 (2007).
20. A. A. Voronin and A. M. Zheltikov, "Soliton-number analysis of soliton-effect pulse compression to single-cycle pulse widths," Phys. Rev. A **78**, 063834 (2008).
21. A. A. Voronin and A. M. Zheltikov, "Soliton self-frequency shift decelerated by self-steepening," Opt. Lett. **33**, 1723–1725 (2008).
22. M. Foster, A. Gaeta, Q. Cao, and R. Trebino, "Soliton-effect compression of supercontinuum to few-cycle durations in photonic nanowires," Opt. Express **13**, 6848–6855 (2005).
23. G. P. Agrawal, *Nonlinear Fiber Optics* (Academic, 2001).
24. P. V. Mamyshev, "Generation and compression of femtosecond solitons in optical fibers," in *Optical Solitons—Theory*

and Experiment, J. R. Taylor, ed. (Cambridge University Press, 1992).
25. W.-h. Cao and P. K. A. Wai, "Picosecond soliton transmission by use of concatenated gain-distributed nonlinear amplifying fiber loop mirrors," Appl. Opt. **44**, 7611–7620 (2005).
26. K. Smith, N. J. Doran, and P. G. J. Wigley, "Pulse shaping, compression, and pedestal suppression employing a nonlinear-optical loop mirror," Opt. Lett. **15**, 1294–1296 (1990).
27. K. Saitoh and M. Koshiba, "Numerical modeling of photonic crystal fibers," J. Lightwave Technol. **23**, 3580–3590 (2005).
28. S. P. Survaiya and R. K. Shevgaonkar, "Design of subpicosecond dispersion-flattened fibers," IEEE Photon. Technol. Lett. **8**, 803–805 (1996).
29. P. Palai, R. K. Varshney, and K. Thyagarajan, "A dispersion flattening dispersion compensating fiber design for broadband dispersion compensation," Fiber Integr. Opt. **20**, 21–27 (2001).
30. T. Yamamoto, H. Kubota, S. Kawanishi, M. Tanaka, and S. Yamaguchi, "Supercontinum generation at 1.55 um in a dispersion-flattened polarization-maintaining photonic crystal fiber," Opt. Express **11**, 1537–1540 (2003).
31. K. Saitoh and M. Koshiba, "Highly nonlinear dispersion-flattened photonic crystal fibers for supercontinuum generation in a telecommunication window," Opt. Express **12**, 2027–2032 (2004).
32. A. Ferrando, E. Silvestre, J. J. Miret, and P. Andrés, "Nearly zero ultraflattened dispersion in photonic crystal fibers," Opt. Lett. **25**, 790–792 (2000).
33. W. H. Reeves, J. C. Knight, and P. St. J. Russell, "Demonstration of ultra-flattened dispersion in photonic crystal fibers," Opt. Express **10**, 609–613 (2002).
34. M. Yan, P. Shum, and C. Lu, "Hole-assisted multiring fiber with low dispersion around 1550 nm," IEEE Photon. Technol. Lett. **16**, 123–125 (2004).
35. W. H. Reeves, D. V. Skryabin, F. Biancalana, J. C. Knight, P. St. J. Russell, F. G. Omenetto, A. Efimov, and A. J. Taylor, "Transformation and control of ultra-short pulses in dispersion-engineered photonic crystal fibres," Nature **424**, 511–515 (2003).